Applied Mathematics & Information Sciences
An International Journal

http://dx.doi.org/10.12785/amis/090210

Towards Human-like Bimanual Movements in Anthropomorphic Robots: A Nonlinear Optimization Approach

E. Costa e Silva[1,2], *M. F. Costa*[3], *J. P. Araújo*[3], *D. Machado*[3], *L. Louro*[3], *W. Erlhagen*[3] *and E. Bicho*[3,*]

[1] CIICESI, ESTGF, Polytechnic Institute of Porto, Portugal
[2] Centre for Mathematics/Dept. of Mathematics and Applications, University of Minho, Portugal
[3] Centre ALGORITMI/Dept. of Industrial Electronics, University of Minho, Portugal

Received: 13 May 2014, Revised: 12 Aug. 2014, Accepted: 14 Aug. 2014
Published online: 1 Mar. 2015

Abstract: Previously we have presented a model for generating human-like arm and hand movements on an unimanual anthropomorphic robot involved in human-robot collaboration tasks. The present paper aims to extend our model in order to address the generation of human-like bimanual movement sequences which are challenged by scenarios cluttered with obstacles. Movement planning involves large scale nonlinear constrained optimization problems which are solved using the IPOPT solver. Simulation studies show that the model generates feasible and realistic hand trajectories for action sequences involving the two hands. The computational costs involved in the planning allow for real-time human robot-interaction. A qualitative analysis reveals that the movements of the robot exhibit basic characteristics of human movements.

Keywords: Large scale nonlinear optimization, IPOPT, bimanual human-like movements, anthropomorphic robot

1 Introduction

One of the ultimate goals in robotics research is to develop robots that are able to work in human-centred environments. Since most tasks and objects in such environments require two hands, it is fundamental that robots are able to perform bimanual tasks, either alone or in collaboration with a human partner. It has been argued that human-robot collaboration is facilitated if the robot has an anthropomorphic shape and shows human-like movements ([1], [2], [3], [4], [5]). These characteristics will support natural and efficient human-robot interaction since they allow the human user to more easily understand the movements of the robot as goal directed actions ([6], [7]). It is thus necessary that a decision of the robot to perform a specific task is translated into bimanual movements that are collision free, fluent, smooth and, most importantly, allow the human co-actor/observer to interpret the underlying motor intention and ultimate action goal.

Endowing anthropomorphic robots with autonomous bimanual object manipulation capabilities is a very complex problem: *i)* First, they have a large number of Degrees of Freedom (DOFs). Even though in biological systems redundancy provides flexibility and the capacity to rapidly compensate for loss of control and adapt to new dynamics, in cognitive robotics controlling multiple DOFs in a predictive/purposive manner is computationally complicated. *ii)* Planning bimanual movements on-line in the context of highly complicated scenarios requires multiple decisions, including which hand does what and how, and close coordination of the movements of the two hands. *iii)* One must guarantee that there is no collision between the two arms-hands and the environment. *iv)* Finally, the problem is exacerbated if the additional goal is to make the robots motor actions look natural to the human.

In the literature there are many recent works on autonomous bimanual manipulation in robotics (e.g.[8],[9]) for a review see [10]). It is a fact that there is still a clear need for the development of new planning and control methods, especially concerning intelligent and human-like bimanual actions in humanoid robots ([11]). One way to go, advocated by us, is the development of

* Corresponding author e-mail: estela.bicho@dei.uminho.pt

anticipatory control processes that at multiple levels (interpersonal space, object space, workspace, joint space) support safe, flexible, adaptive and human-like bimanual action sequences. In order to implement effective and human-like actions we focus here on anticipatory aspects of movement planning that characterize intelligent human behaviour ([12], [13], [14]). Intelligent behaviour is inherently tuned to reach future goal states. The relative positions of the hands on the object sets the conditions for the forthcoming movements and thus affects what can ultimately be done with the object. For instance, in the planning of (uni and bimanual) goal-directed movements, the decision on how to grasp the object essentially depends on the (anticipated) final goal, the intention of the action. In previous work [15], we have presented a computational model for real-time generation of smooth and human-like goal-directed movements on an uni-manual anthropomorphic robot involved in human-robot collaboration tasks (see [16] for examples on these tasks). The model is strongly inspired by the Posture-Based Motion Planning Model (PBMPM) of Rosenbaum and colleagues (e.g. [12], [17]) which was proposed to explain how humans plan goal-directed upper limb movements. In our view the PBMPM model is interesting for the robotics domain as well. It enables to address the anticipatory aspect of intelligent movement planning, by allowing to impose a particular grip type that was selected based on the ultimate goal of what to do with the object. It permits to address the motor redundancy problem by first selecting a final goal posture (that allows the object to be grasped with the desired grip type) and subsequently the selection of an efficient trajectory that takes into account several task constraints (e.g. obstacle avoidance). Finally, the model allows to implement and generate important features observed in human upper-limb movements (e.g. minimum jerk, bell-shape velocity profiles for the joints, joints synchrony). In our implementation, the selection processes have been formalized as nonlinear constraint optimization problems.

The present paper aims to extend our model in order to address the generation of human-like bimanual movement sequences which are challenged by scenarios cluttered with obstacles.
Although the use of optimization in the generation of robot movements is not new (see e.g. [18]), roboticists have paid little attention to the large amount of available optimization software (see e.g. https://projects.coin-or.org/) and to the underlying optimization techniques. In general the optimization problems that arise from the generation of robot movements are large ones.

Pattacini et al [19] used IPOPT[1] to solve the inverse kinematics problem of an anthropomorphic robotics arm in point-to-point movements in the absence of obstacles. In [21] IPOPT is used to find an optimal weight vector that minimizes the deviations between recorded human data and the quantities corresponding to the solution of an optimal control problem with equality constraints. A computational approach for transferring principles of human motor control to humanoid robots is presented in [22]. The authors determine the optimal trajectories by solving a nonlinear programming problem that is encoded by using a basis of motor primitives.

However, in all above mentioned works, based on optimization, only unimanual reaching movements have been addressed and obstacle avoidance was not considered.

With the present paper we intent to make a step forward. Specifically, we model the entire human-like trajectory of both arms and hands of the anthropomorphic robot, including obstacle avoidance. The nonlinear constrained optimization problems that arise in this modelling are large ones. The large dimensions of these problems are related to the discretization of the time-dependent functions, and with the number of the obstacles that exist in the workspace of the robot. To solve the optimization problems we use IPOPT. There are two reasons for this choice. First, it is adequate for solving very large scale optimization problems. Second, in previous work [23] we have shown that IPOPT solver is very efficient and robust for generating human-like collision free trajectories. Very important, it was able to find optimal solutions in CPU times small enough to allow it to be integrate in the movement planning system for real-time human-robot interactions.

The rest of the paper is organized as follows. Section 2 gives an overview of our model for planning human-like bimanual movements and its formalization as a nonlinear constrained optimization problem. Section 3 presents results obtained in our MATLAB simulator of the Anthropomorphic Robot **ARoS** performing a construction task that requires the use of the two hands, and which is challenged by the presence of several obstacles. Finally, Section 4 is devoted to conclusions and an outlook for future work.

2 The model

The robot has two anthropomorphic arms and hands. Each anthropomorphic redundant robotic arm and hand can be represented as a series of links connected by joints. The number of joints which can be independently

[1] IPOPT [20] is an open source software package for large scale nonlinear optimization, that implements a primal-dual interior point filter line search method for solving nonlinear constrained large-scale optimization problems.

actuated define its DOFs. Each of **ARoS**' anthropomorphic robotic arm has 7 DOFs, $\theta_1^a,\ldots,\theta_7^a$, and each hand has 4 DOFs, $\theta_8^a,\ldots,\theta_{11}^a$. Therefore, the arm and hand configuration in joint space is defined by the vector

$$\boldsymbol{\theta}^a = (\theta_1^a,\theta_2^a,\ldots,\theta_{11}^a)^\top, \tag{1}$$

where $a = R$ or $a = L$, for the right or left arm and hand, respectively.

Taking inspiration from the PBMP model [12], we define the movement of each joint as the superimposition of two movements:

(i) a *direct movement*, describing a bell-shaped unimodal velocity profile, from the initial to final posture;
(ii) a *back-and-forth movement* from initial to a bounce posture, intended to avoid collision with obstacles in the robot's workspace.

In general, the movement planning of each arm and hand involves the resolution of two problems:

Pa determining the appropriate final posture, i.e., a vector of arm and hand joint angles, $\boldsymbol{\theta}_f^a \in \mathbb{R}^{n_j^a}$, that allows, for e.g., **ARoS** to grasp a given object or to achieve a specific location, with a particular grip type;
Pb determining a bounce posture, $\boldsymbol{\theta}_b^a \in \mathbb{R}^{n_j^a}$, that serves as a sub-goal for a *back-and-forth* movement, with the intent of yielding a collision-free movement from start to end.

Here $n_j^a = 7,\ldots,11$ is the number of joints, with $a \in \{R,L\}$, depends on the type of movement (see Subsection 2.2). Problems **Pa** and **Pb** were modelled as nonlinear constrained optimization problems, with bounds, equality and inequality constraints. For defining the constraints of these optimization problems we use the direct kinematics expressions that are presented in the next subsection, which is followed by the formulation of the optimization problems.

2.1 Arms and hands kinematics

For the direct kinematics of the robotic arm and hand well known Denavit-Hartenberg parameters are used (see Table 1 for the parameters used). For further information on kinematics of robotic arm see e.g. [24].

The 3D Cartesian coordinates and orientation of the points in the arm and hand, $a \in \{R,L\}$, relatively to a world reference frame, are written as functions of the arm and hand joint angles using the direct kinematics transformation:

$${}_7^W T^R = {}_7^0 T \text{ and } {}_7^W T^L = T\,{}_7^0 T, \tag{2}$$

Table 1: Denavit-Hartenberg parameters for the 7 DOFs robotic arm and for each k finger of the robotic hand ($k = 1,2,3$). Here $a \in \{R,L\}$, $r = (-1,1,0)^\top$ and $j = (-1,-1,1)^\top$; $L_1^a, L_u^a, L_l^a, L_h^a$ are arm specific parameters and $A_1, A_2, A_3, D_3, \phi_2, \phi_3$ are hand specific parameters.

i	α_{i-1} (deg)	a_{i-1} (mm)	d_i (mm)	θ_i (deg)
1	90	0	L_1^a	θ_1^a
2	90	0	0	θ_2^a
3	-90	0	L_u^a	θ_3^a
4	90	0	0	θ_4^a
5	-90	0	L_l^a	θ_5^a
6	90	0	0	θ_6^a
7	-90	0	L_h^a	θ_7^a
k,8	0	$r_k A_w$	0	$r_k\,\theta_{11}^a - 90\,j_k$
k,9	90	A_1	0	$\phi_2 + \theta_{7+k}^a$
k,10	0	A_2	0	$\phi_3 + \frac{1}{3}\theta_{7+k}^a$
k,11	-90	A_3	D_3	0

where ${}_7^0 T = {}_1^0 T\,{}_2^1 T\,{}_3^2 T\,{}_4^3 T\,{}_5^4 T\,{}_6^5 T\,{}_7^6 T$, $T = \begin{pmatrix} 1 & 0 & 0 & 0 \\ 0 & -1 & 0 & 100 \\ 0 & 0 & -1 & 0 \\ 0 & 0 & 0 & 1 \end{pmatrix}$

and ${}_i^{i-1} T = \begin{pmatrix} c_i & -s_i & 0 & a_{i-1} \\ s_i\,c^{i-1} & c_i\,c^{i-1} & -s^{i-1} & -s^{i-1}\,d_i \\ s_i\,s^{i-1} & c_i\,s^{i-1} & c^{i-1} & c^{i-1}\,d_i \\ 0 & 0 & 0 & 1 \end{pmatrix}$,

is the transformation matrix from frame $i-1$ to frame i, where $c_i = \cos(\theta_i)$, $s_i = \sin(\theta_i)$, $c^{i-1} = \cos(\alpha_{i-1})$, $s^{i-1} = \sin(\alpha_{i-1})$.

Note that, the direct kinematics transformation of the left arm is the same as the one of the right arm except for the pre-multiplication by T that describes the difference between the position and orientation of the left arm relatively to the right arm.

Using (2) it is possible to determine the position, and orientation, of each point in the arms as a nonlinear function of the joint angles. For example, for the right arm, the position of the center of the shoulder, $\boldsymbol{S}^R$, elbow, $\boldsymbol{E}^R$, wrist, $\boldsymbol{W}^R$, and tip of hand, $\boldsymbol{H}^R$, are given by:

$$\boldsymbol{S}^R(\boldsymbol{\theta}^R) = \begin{pmatrix} 0 \\ -L_1^R \\ 0 \end{pmatrix}, \boldsymbol{E}^R(\boldsymbol{\theta}^R) = \begin{pmatrix} -c_1^R s_2^R L_u^R \\ -c_2^R L_u^R - L_1^R \\ -s_1^R s_2^R L_u^R \end{pmatrix},$$

$$\boldsymbol{W}^R(\boldsymbol{\theta}^R) = \begin{pmatrix} \delta_2 L_l^R - c_1^R s_2^R L_u^R \\ \beta_5 L_l^R - c_2^R L_u^R - L_1^R \\ \delta_4 L_l^R - s_1^R s_2^R L_u^R \end{pmatrix},$$

$$\boldsymbol{H}^R(\boldsymbol{\theta}^R) = \begin{pmatrix} (-(\delta_1 c_5^R - \beta_3 s_5^R)s_6^R + \delta_2 c_6^R)L_h^R + \delta_2 L_l^R - c_1^R s_2^R L_u^R \\ (-\delta_5 s_6^R + \beta_5 c_6^R)L_h^R + \beta_5 L_l^R - c_2^R L_u^R - L_1^R \\ (-(\delta_3 c_5^R - \beta_4 s_5^R)s_6^R + \delta_4 c_6^R)L_h^R + \delta_4 L_l^R - s_1^R s_2^R L_u^R \end{pmatrix},$$

where

$$\begin{aligned}
\beta_1 &= c_1^R c_2^R c_3^R - s_1^R s_3^R, \quad \beta_2 = s_1^R c_2^R c_3^R + c_1^R s_3^R,\\
\beta_3 &= c_1^R c_2^R s_3^R + s_1^R c_3^R, \quad \beta_4 = s_1^R c_2^R s_3^R - c_1^R c_3^R,\\
\beta_5 &= s_2^R c_3^R s_4^R - c_2^R c_4^R, \quad \beta_6 = -s_2^R c_3^R c_4^R - c_2^R s_4^R,\\
\delta_1 &= \beta_1 c_4^R - c_1^R s_2^R s_4^R, \quad \delta_2 = -\beta_1 s_4^R - c_1^R s_2^R c_4^R,\\
\delta_3 &= \beta_2 c_4^R - s_1^R s_2^R s_4^R, \quad \delta_4 = -\beta_2 s_4^R - s_1^R s_2^R c_4^R,\\
\delta_5 &= \beta_6 c_5^R + s_2^R s_3^R s_5^R, \quad \delta_6 = \beta_6 s_5^R - s_2^R s_3^R c_5^R,
\end{aligned}$$

The hand orientation can be described by the orientation of local frame $\hat{\boldsymbol{x}}_7^R \hat{\boldsymbol{y}}_7^R \hat{\boldsymbol{z}}_7^R$, whose principal axes are functions of the joint angles:

$$\hat{\boldsymbol{x}}_7^R(\boldsymbol{\theta}^R) = \begin{pmatrix} (((\delta_1 c_5^R - \beta_3 s_5^R) c_6^R + \delta_2 s_6^R) c_7^R - (\delta_1 s_5^R + \beta_3 c_5^R) s_7^R \\ (\delta_5 c_6^R + \beta_5 s_6^R) c_7^R - \delta_6 s_7^R \\ (((\delta_3 c_5^R - \beta_4 s_5^R) c_6^R + \delta_4 s_6^R) c_7^R - (\delta_3 s_5^R + \beta_4 c_5^R) s_7^R \end{pmatrix},$$

$$\hat{\boldsymbol{y}}_7^R(\boldsymbol{\theta}^R) = \begin{pmatrix} -(((\delta_1 c_5^R - \beta_3 s_5^R) c_6^R + \delta_2 s_6^R) s_7^R - (\delta_1 s_5^R + \beta_3 c_5^R) c_7^R \\ -(\delta_5 c_6^R + \beta_5 s_6^R) s_7^R - \delta_6 c_7^R \\ -(((\delta_3 c_5^R - \beta_4 s_5^R) c_6^R + \delta_4 s_6^R) s_7^R - (\delta_3 s_5^R + \beta_4 c_5^R) c_7^R \end{pmatrix},$$

and

$$\hat{\boldsymbol{z}}_7^R(\boldsymbol{\theta}^R) = \begin{pmatrix} -(\delta_1 c_5^R - \beta_3 s_5^R) s_6^R + \delta_2 c_6^R \\ -\delta_5 s_6^R + \beta_5 c_6^R \\ -(\delta_3 c_5^R - \beta_4 s_5^R) s_6^R + \delta_4 c_6^R \end{pmatrix}.$$

Analogously, we obtain the nonlinear functions that allow to determine the position and orientation of points in the left arm and also for points in both the right and the left robotic hands.

2.2 Problem formulation

For each robotic arm and hand $a \in \{R, L\}$, the trajectory of the joint angles is given by

$$\begin{aligned}
\boldsymbol{\theta}^a(t) &= \mathscr{T}^a(t, \boldsymbol{\theta}_f^a, \boldsymbol{\theta}_b^a)\\
&= \boldsymbol{\theta}_0^a + \mathscr{T}_{direct}^a(t, \boldsymbol{\theta}_f^a) + \mathscr{T}_{bk}^a(t, \boldsymbol{\theta}_b^a). \qquad (3)
\end{aligned}$$

$\mathscr{T}_{direct}^a$ is the direct movement which consists of a trajectory based on the minimum angular jerk principle, i.e. the minimization of the change of angle acceleration. This implies minimizing the integration of the jerk over the movement duration. This is a typical variational problem, solved using the Euler-Poison equation. The solution is a 5^{th} order polynomial whose coefficients may be determined applying boundary conditions on position, velocity and acceleration. Assuming that the movement starts and ends with zero velocity and acceleration, the solution to this minimization problem is,

$$\mathscr{T}_{direct}^a(t, \boldsymbol{\theta}_f^a) = (\boldsymbol{\theta}_f^a - \boldsymbol{\theta}_0^a)\left(10\tau^3 - 15\tau^4 + 6\tau^5\right). \qquad (4)$$

$\mathscr{T}_{bk}^a(t, \boldsymbol{\theta}_b^a)$ is the back-and-forth movement imposed to avoid collision with obstacles, which is modelled as

$$\mathscr{T}_{bk}^a(t, \boldsymbol{\theta}_b^a) = (\boldsymbol{\theta}_b^a - \boldsymbol{\theta}_0^a)\sin^2(\pi\,\tau^{\vartheta}). \qquad (5)$$

In (4) and (5), $\tau = \frac{t}{T_\mathrm{d}} \in [0,1]$ is the normalized movement duration, $T_\mathrm{d} \in \mathbb{R}^+$ represents the movement duration, $t \in [0, T_\mathrm{d}]$, and $\vartheta = -\frac{\ln 2}{\ln t_b}$, $t_b \in]0,1[$ is the movement time when the bounce posture is applied.

Next, we explain how to compute $\boldsymbol{\theta}_f^a$ and $\boldsymbol{\theta}_b^a$.

We use a direct transcription method, therefore, $t \in [0, T_\mathrm{d}]$ is discretized in N_T equally spaced points $t_i = i\Delta$, where $\Delta = \frac{T_\mathrm{d}}{N_T}$ is the step size and $i = 0, 1, \ldots, N_T$. Our convention is that $\mathscr{T}_i^a \equiv \mathscr{T}^a(t_i, \boldsymbol{\theta}_f, \boldsymbol{\theta}_b)$ represents $\mathscr{T}^a(t, \boldsymbol{\theta}_f, \boldsymbol{\theta}_b)$ at time t_i.

We start by computing the joints of the hand, $\theta_8^a, \ldots, \theta_{11}^a$, resorting to the inverse kinematics. The movement planning system receives information about the desired grip type (how to grasp the object), the location and orientation of the target object and its physical dimensions. For a successful grasp, the following simplifications are possible. First, we consider that the middle finger is opposite to the other two, therefore $\theta_{f,8}^a = 0$. Second, since all fingers have equal lengths, we set $\theta_{f,9}^a = \theta_{f,10}^a = \theta_{f,11}^a$. Thus, given the geometry of the hand, a specific object and grip type, the joint angles of the fingers $\theta_{f,9}^a$ are determined by solving

$$\begin{aligned}
A_3\cos(\frac{4}{3}\theta_{f,9}^a + \phi_2 + \phi_3) - D_3\sin(\frac{4}{3}\theta_{f,9}^a + \phi_2 + \phi_3)\\
+A_2\cos(\theta_{f,9}^a + \phi_2) + A_1\\
= \frac{d_{obj}}{2},
\end{aligned}$$

using the Newton-Raphson method. Here d_{obj} is the object diameter, and $A_1, A_2, A_3, D_3, \phi_2, \phi_3$ are hand specific parameters[2].

After the joint angles of the hand have been computed we proceed with the computation of the final posture of the arm $\theta_{f,1}^a, \ldots, \theta_{f,7}^a$, for the left or right arm. The aim is to select the optimal end posture that minimizes the displacement of the joints from the initial to the final posture, taking into account obstacle avoidance, joint limits and grip type, at the moment of grasp. Mathematically we formulate the problem as follows:

$$\mathbf{Pa}^a \min_{\theta_1^a, \ldots, \theta_7^a} \sum_{k=1}^{7} \left(\theta_{0,k}^a - \theta_{f,k}^a\right)^2 \qquad (6)$$

$$\text{s.t.} \quad \boldsymbol{h}_1^a(\theta_{f,1}^a, \ldots, \theta_{f,7}^a, \theta_{f,9}^a) = \mathbf{0} \qquad (7)$$

$$\boldsymbol{h}_2^a(\theta_{f,1}^a, \ldots, \theta_{f,7}^a) = \mathbf{0} \qquad (8)$$

$$\boldsymbol{h}_f^a(\theta_{f,1}^a, \ldots, \theta_{f,11}^a) \leq \mathbf{0} \qquad (9)$$

$$\theta_{m,i}^a \leq \theta_{f,i}^a \leq \theta_{M,i}^a, \qquad i = 1, \ldots, 7 \qquad (10)$$

where $\theta_{m,i}^a$ and $\theta_{M,i}^a$ are constants that represent the lower and upper joint limits of each arm $a \in \{R, L\}$ respectively; $\boldsymbol{h}_1^a$ and $\boldsymbol{h}_2^a$ are nonlinear functions (of target pose and joint angles) concerning the position and orientation of the robot hand relatively to the target, respectively; $\boldsymbol{h}_f^a$ are

[2] $A_1 = 50\,mm$, $A_2 = 70\,mm$, $A_3 = 50\,mm$, $D_3 = 9.5\,mm$, $\phi_2 = 2.46\,deg$, $\phi_3 = 50\,deg$.

nonlinear functions of the obstacles pose and arm-hand angles, and is concerned with collision avoidance at the moment of grasp, with all the obstacles in the workspace.

Now that $\boldsymbol{\theta}_f^a$ has been found, the bounce posture $\boldsymbol{\theta}_b^a$ can be selected. The aim is to select the optimal bounce posture that minimizes the displacement of the joints from the initial to the bounce posture, subject to obstacle avoidance and joint limits, over the entire duration of the movement:

$$\mathbf{Pb}^a \min_{\theta_{b,1}^a,\dots,\theta_{b,n_j^a}^a} \sum_{k=1}^{n_j^a} \left(\theta_{0,k}^a - \theta_{b,k}^a\right)^2 \tag{11}$$

$$\text{s.t.} \quad \boldsymbol{\theta}_m^a \le \mathscr{T}^a(t_i, \boldsymbol{\theta}_f^a, \boldsymbol{\theta}_b^a) \le \boldsymbol{\theta}_M^a \tag{12}$$

$$\underline{\boldsymbol{h}}_b^a(\mathscr{T}^a(t_i, \boldsymbol{\theta}_f^a, \boldsymbol{\theta}_b^a)) \le \mathbf{0} \tag{13}$$

$$\overline{\boldsymbol{h}}_b^a(\mathscr{T}^a(t_i, \boldsymbol{\theta}_f^a, \boldsymbol{\theta}_b^a), \varepsilon(t_i)) \le \mathbf{0}, \tag{14}$$

$$\boldsymbol{\theta}_m^a \le \boldsymbol{\theta}_b^a \le \boldsymbol{\theta}_M^a \tag{15}$$

$$t_i = 0, \dots, T_\mathrm{d}$$

where $\boldsymbol{\theta}_m^a$ and $\boldsymbol{\theta}_M^a$ are constant vectors that represent the lower and upper joint limits of each arm-hand $a \in \{R, L\}$, $\varepsilon(t_i)$ is a function of time representing the clearance distance, and $\underline{\boldsymbol{h}}_b^a, \overline{\boldsymbol{h}}_b^a$ are nonlinear functions of the obstacles pose and of the arm-hand angles. $\underline{\boldsymbol{h}}_b^a$ represents collision avoidance for all the time instants in the movement. Finally, $\overline{\boldsymbol{h}}_b^a$ deals with collision avoidance with the object to be grasped.

In general, depending on the type of movement, the movement planning of each arm and hand:
(i) can involve only one of the problems $\mathbf{Pa}^a$ or $\mathbf{Pb}^a$,
(ii) the number of joints used in the movement planning can be different,
(iii) the obstacle avoidance constraints need to be adjusted.

For instance:

- *reach-to-grasp* movements consist of one $\mathbf{Pa}^a$ and one $\mathbf{Pb}^a$ problems with $n_j^a = 9$.
- *transporting and placing* an object do not allow movements of the fingers (since the robot is holding the object), thus for $\mathbf{Pb}^a$ $n_j^a = 7$. In this case the movement is composed of two sub-movements:
  - the first from the initial posture to some location behind the insertion point;
  - the second from this location to the insertion point (this is a direct movement).

  Therefore these type of movements consists of two $\mathbf{Pa}^a$ problems $\mathbf{Pa}_1^a$ for determining the pose of arm at the insertion point, and $\mathbf{Pa}_2^a$ for location behind the insertion point and one $\mathbf{Pb}^a$ problem.

For tasks that require sequences of movements involving both arm-hands, e.g. 'reach→grasp→regrasp→place', an action planner gives the desired intermediate goals (grip types) for both hands. The initial posture of the second arm-hand is defined by the end posture of the first arm-hand.

2.3 Constraints specifications

For constraints (7) and (8) in $\mathbf{Pa}^a$ we have:

$$\begin{aligned}&\boldsymbol{h}_1^a(\theta_{f,1}^a, \dots, \theta_{f,7}^a, \theta_{f,9}^a)\\ &= \boldsymbol{H}^a(\theta_{f,1}^a, \dots, \theta_{f,7}^a) + d_{HO}(\theta_{f,9}^a)\, \hat{\boldsymbol{z}}_7^a(\theta_{f,1}^a, \dots, \theta_{f,7}^a) - \boldsymbol{X}_{tar},\end{aligned}$$

$$\boldsymbol{h}_2^a(\theta_{f,1}^a, \dots, \theta_{f,7}^a) = \hat{\boldsymbol{x}}_7^a(\theta_{f,1}^a, \dots, \theta_{f,7}^a) - \hat{\boldsymbol{z}}_{tar},$$

where $d_{HO}(\theta_{f,9}^a) = A_3 \sin(\frac{4}{3}\theta_{f,9}^a + \phi_2 + \phi_3) + D_3 \cos(\frac{4}{3}\theta_{f,9}^a + \phi_2 + \phi_3) + A_2 \sin(\theta_{f,9}^a + \phi_2)$, $\boldsymbol{X}_{tar}$ is the target position, $\hat{\boldsymbol{z}}_{tar} = (s\phi s\gamma + c\phi s\psi c\gamma, -c\phi s\gamma + s\psi s\phi c\gamma, c\psi c\gamma)^\top$, ϕ, ψ, γ are the euler angles giving the orientation of the target. Therefore, we have 4 constraints in (7) and (8).

For the obstacle avoidance constraints in $\mathbf{Pa}^a$ and $\mathbf{Pb}^a$ problems, (i.e. (9), (13), (14)) we model each arm and hand by spheres, the torso as an elliptic cylinder and the obstacles as ellipsoids.

Let $n_{obj} \in \mathbb{N}_0$ be the number of obstacles in the robot's workspace, $\boldsymbol{C}_l$ and $r_{x,l}$, $r_{y,l}$, $r_{z,l}$, $\phi_l, \psi_l, \gamma_l, l = 1, \dots, n_{obj}$ be their centers, dimensions in its main three axis and orientation, respectively. Additionally, let $\boldsymbol{P}_k^a(\boldsymbol{\theta}) = (P_{k,1}^a(\boldsymbol{\theta}), P_{k,2}^a(\boldsymbol{\theta}), P_{k,3}^a(\boldsymbol{\theta}))^\top$, $k = 1, \dots, 15$, be the centers of the 15 spheres on each robotic arm and hand $a \in \{R, L\}$ whose radius are r_k^a.

The inequality constraints (9) are due to obstacle avoidance, namely, collision between:

(1) body/torso of the robot and its arms and hands;
(2) arms and hands of the robot and the table;
(3) obstacles in the workspace of the robot and its arms and hands;
(4) the left and the right arm and hand;

whose constraints functions are defined by:

$$h_{f,1}^{a,k} = 1 - \left(\frac{P_{k,1}^a(\boldsymbol{\theta}_f^a) - x_0}{\sigma_x}\right)^2 - \left(\frac{P_{k,2}^a(\boldsymbol{\theta}_f^a) - y_0}{\sigma_y}\right)^2,$$

$$h_{f,2}^{a,k} = r_k^a + h_{table} - P_{k,3}^a(\boldsymbol{\theta}_f^a),$$

$$\begin{aligned}h_{f,3}^{a,\bar{k}} &= 1 - (\boldsymbol{P}_k^a(\boldsymbol{\theta}_f^a) - \boldsymbol{C}_l)^\top \boldsymbol{R}_l^\top \boldsymbol{A}_{l,k} \boldsymbol{R}_l (\boldsymbol{P}_k^a(\boldsymbol{\theta}_f^a) - \boldsymbol{C}_l),\\ &\quad k = 1, \dots, 15,\\ &\quad l = 1, \dots, n_{obj},\end{aligned}$$

$$\begin{aligned}h_{f,4}^{a,\hat{k}} &= r_{k^R}^R + r_{k^L}^L - \|\boldsymbol{P}_{k^R}^R(\boldsymbol{\theta}_f^R) - \boldsymbol{P}_{k^L}^L(\boldsymbol{\theta}_f^L)\|,\\ &\quad k^R = 1, \dots, 15,\\ &\quad k^L = 1, \dots, 15,\end{aligned}$$

where $k = 1, \dots, 15$, $\bar{k} = 1, \dots, 15 \times n_{obj}$, $\hat{k} = 1, \dots, 15 \times 15$, (x_0, y_0) is the position of the torso of the robot, σ_x and σ_y are its dimensions, h_{table} is the height of the table, $\boldsymbol{A}_{l,k} = (\mathrm{diag}(r_{x,l}, r_{y,l}, r_{z,l}) + (r_k + \varepsilon)I)^{-2}$, $\boldsymbol{R}_l = \boldsymbol{R}_l(\phi_l, \psi_l, \gamma_l)$ is the matrix given the orientation of object l. Therefore, in (9)

Table 2: Problems description.

Movement	Arm-hand	Final Posture Selection	Bounce Posture Selection
1	left	$\mathbf{P1a}^L$	$\mathbf{P1b}^L$
2	left	-	$\mathbf{P2b}^L$
3	right	$\mathbf{P3a}^R$	$\mathbf{P3b}^R$
4	right	$\mathbf{P4a}_1^R$+$\mathbf{P4a}_2^R$	$\mathbf{P4b}^R$

$\boldsymbol{h}_f^a(\boldsymbol{\theta}_f^a) = \left(\boldsymbol{h}_{f,1}^a, \boldsymbol{h}_{f,2}^a, \boldsymbol{h}_{f,3}^a, \boldsymbol{h}_{f,4}^a\right)^\top$. In conclusion, for problem $\mathbf{Pa}^a$, expressions (7), (8), (9), (10), give rise to a total number of $15 \times (18 + n_{obj}) + 20$ constraints.

The inequality constraints (13) are also due to obstacle avoidance, as explained above, but now for each instant time t_i. The vector of the functions constraints is $\underline{\boldsymbol{h}}_b^a(\mathscr{T}_i^a) = \left(\underline{\boldsymbol{h}}_{b,1,i}^a, \underline{\boldsymbol{h}}_{b,2,i}^a, \underline{\boldsymbol{h}}_{b,3,i}^a, \underline{\boldsymbol{h}}_{b,4,i}^a\right)^\top$ where

$$\underline{\boldsymbol{h}}_{b,1,i}^{a,k} = 1 - \left(\frac{P_{k,1}^a(\mathscr{T}_i^a) - x_0}{\sigma_x}\right)^2 - \left(\frac{P_{k,2}^a(\mathscr{T}_i^a) - y_0}{\sigma_y}\right)^2,$$

$$\underline{\boldsymbol{h}}_{b,2,i}^{a,k} = r_k^a + h_{table} - P_{k,3}^a(\mathscr{T}_i^a),$$

$$\underline{\boldsymbol{h}}_{b,3,i}^{a,k,l} = 1 - (\boldsymbol{P}_k^a(\mathscr{T}_i^a) - \boldsymbol{C}_l)^\top \boldsymbol{R}_l^\top \boldsymbol{A}_{l,k} \boldsymbol{R}_l (\boldsymbol{P}_k^a(\mathscr{T}_i^a) - \boldsymbol{C}_l),$$
$$k = 1, \ldots, 15,$$
$$i = 1, \ldots, N_T,$$
$$l = 1, \ldots, n_{obj},$$

$$\underline{\boldsymbol{h}}_{b,4,i}^{a,k^R,k^L} = r_{k^R} + r_{k^L} - \|\boldsymbol{P}_{k^R}^R(\mathscr{T}_i^R) - \boldsymbol{P}_{k^L}^L(\mathscr{T}_i^L)\|,$$
$$k^R, k^L = 1, \ldots, 15,$$
$$i = 1, \ldots, N_T,$$

which implies a total of $15 \times (18 + n_{obj}) \times N_T$ constraints in (13).

Finally, for the inequality constraints (14) we have

$$\overline{\boldsymbol{h}}_b^a(\mathscr{T}_i^a) = 1 - (\boldsymbol{P}_k^a(\mathscr{T}_i^a) - \boldsymbol{X}_{tar})^\top \boldsymbol{R}_{tar}^\top \boldsymbol{A}_{tar,k,i} \boldsymbol{R}_{tar} (\boldsymbol{P}_k^a(\mathscr{T}_i^a) - \boldsymbol{X}_{tar}),$$

where $\boldsymbol{A}_{tar,k,i} = \text{diag}((r_k + r_{x,t_i} + \varepsilon(t_i))^{-2}, (r_k + r_{y,t_i} + \varepsilon(t_i))^{-2}, (r_k + r_{z,t_i} + \varepsilon(t_i))^{-2})$, $k = 1, \ldots, 15$ and $i = 1, \ldots, N_T$. This gives $15 \times N_T$ constraints for (14).

Therefore, for solving problem $\mathbf{Pb}^a$, expressions (13) , (14), (12), (15), held a total of $15N_T \times (19 + n_{obj}) + 2n_{obj} \times (N_T + 1)$ constraints.

3 Results

The results concern movements involved in a construction task of a toy "vehicle" from components that are initially distributed on a table (c.f. Figure 1). The dual-arm robot **ARoS** needs to assemble a "vehicle" consisting of a round base with an axle on which two wheels have to be attached and then fixed with a nut. Subsequently four different columns have to be plugged into specific holes in the platform. For further details on this construction task, and involving human-robot joint action, see [6][7].

Here we focus on the sub-task in which the robot has to transport an object laterally, from one side of the workspace to the other, in the presence of obstacles. The task requires the robot to pick up a target object with one hand, transporting it to the other hand, and transporting the object with the other hand to the target position at the opposite side of the workspace. Specifically, we present results on a sequence of movements that involve both arm-hands:

Movement 1 - Reaching and Grasping a column from the table with the left arm;
Movement 2 - Transporting the column from the left to the right hand;
Movement 3 - Reaching and grasping the column using the right hand;
Movement 4 - Transporting the column and plugging it into a specific hole in the round base.

All optimization problems, $\mathbf{P\#a}^a$ and $\mathbf{P\#b}^a$ ($a \in \{R, L\}$), were coded in AMPL modeling language and solved using IPOPT 3.11. The numerical results were obtained using a core i7-4770 - 3.4GHz, 8Gb de RAM, and graphic card AMD Radeon 6570HD - 1GB DDR3. In our implementation the value of the following constants are: $T_\text{d} = 1$ and $t_b = 0.5$. IPOPT was run with the default options, with the exception of the second order derivatives information that were approximated using a limited-memory Broyden - Fletcher - Goldfarb - Shanno method and that we set AMPL presolve off. In practice the equality constraints were transformed into inequality constrained considering its squared euclidean norm and using $\delta = 10^{-3}$.

The numerical results are presented in Tables 3 and 4, which contain the number of variables, N, the total number of constraints, M, the optimal objective function value, Obj*, and the computational time in seconds, CPU.

Table 3: Numerical results for $\mathbf{Pa}^a$ problems.

	$\mathbf{P1a}^L$	$\mathbf{P3a}^L$	$\mathbf{P4a}_1^R$	$\mathbf{P4a}_2^R$
N	7	7	7	7
M	92	92	81	81
Obj*	8.148	2.898	0.685	0.054
CPU	0.112	0.165	0.3180	0.210

Table 4: Numerical results for $\mathbf{Pb}^a$ problems.

	$\mathbf{P1b}^L$	$\mathbf{P2b}^L$	$\mathbf{P3b}^R$	$\mathbf{P4b}^R$
N_T	20	20	10	20
N	9	7	9	7
M	1806	1022	701	1324
Obj*	0.026	0.111	9×10^{-14}	0.03
CPU	2.022	1.104	0.219	1.297

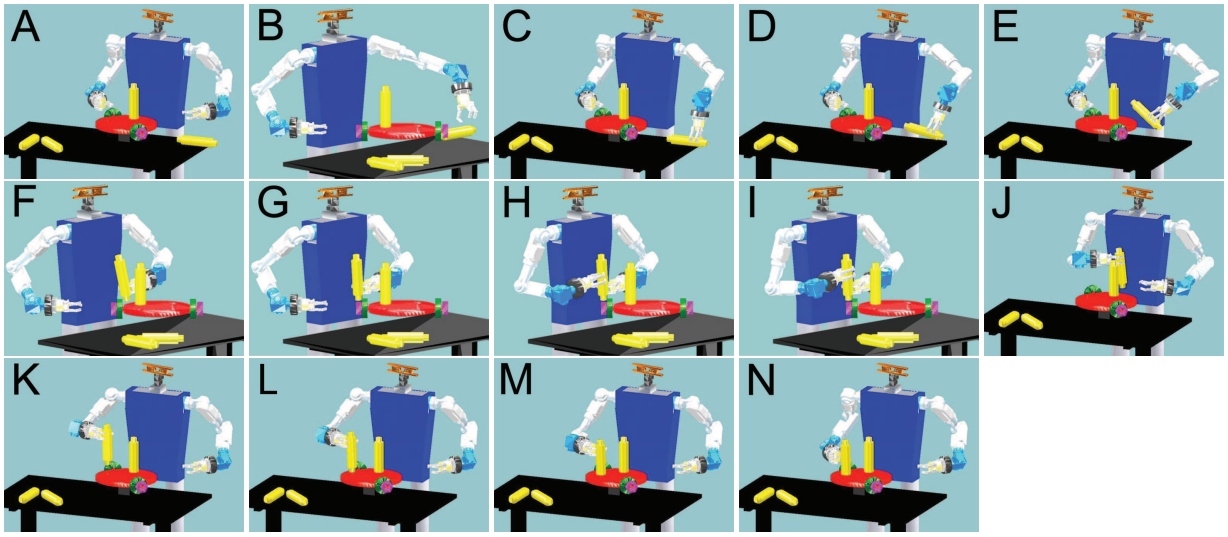

Fig. 1: Snapshots, in our MATLAB simulator, of **ARoS** performing the sequence of movements 'reach→grasp→regrasp→place'.

ARoS starts and ends this sequence of movements with the left arm in its home position for which the joint angles are $(137,-78,-106,-95,43,-64,132,0,70,70,70)^\top$ (deg) and for the right arm the home position is $(-137,-78,106,-95,-43,-64,48,0,70,70,70)^\top$ (deg).

The $\mathbf{Pa}^a$ are small scale optimization problems. For Movement 1 (i.e. $\mathbf{P1a}^L$ problem), IPOPT found an optimal solution in less than 0.12 seconds. This solution allows **ARoS** to successfully grasp, with the left hand, the column that is placed on the table (Snapshot (C) in Figure 1). In less than 0.17 seconds the solver found an optimal solution for the final posture in Movement 3 (i.e. $\mathbf{P3a}^R$ problem). It corresponds to a posture that allows **ARoS** to grasp with the right hand the column that has been transported by the left hand (Snapshot (I) in Figure 1). For Movement 4, two $\mathbf{Pa}^R$ were solved successfully. The posture for plugging the column in the round base, which is the solution of $\mathbf{P4a}_2^R$ (Snapshot (M) in Figure 1) took 0.21 seconds, while computing the posture that places the object in the location behind the insertion point, $\mathbf{P4a}_1^R$, took less than 0.32 seconds (Snapshot (L) in Figure 1).

The $\mathbf{Pb}^a$ are large scale optimization problems. For all the solver found optimal solutions. Problem $\mathbf{P1b}^L$ was the one whose solution took more time to be found. This is essentially due to two reasons: it is the largest optimization problem and Movement 1 presents the greater risk of collision with the surrounding obstacles. (Snapshots (A), (B), (C) in Figure 1). In particular it involves the preshaping of the fingers aperture for grasping the column without colliding with it. And also, the hand must be very close to the table.

For Movement 2 (i.e problem $\mathbf{P2b}^L$) the selection of the bounce posture took less than 1.2 seconds. This is a transporting movement therefore there is no movements of the joints of the fingers (See Figure 2). The main challenge for this movement is that the obstacle avoidance constraints include also the collision between the column that is transported by the hand and all the surrounding obstacles.

Movement 3 (Snapshots (G), (H), (I) in Figure 1) is the one that presents the smaller risk of collision. Although it is a reach to grasp movement, which involves a preshaping of the fingers, it is the smallest of the $\mathbf{Pb}^a$ problems. In fact, it involves a small distance to be travelled by the hand and it is performed in a region of the workspace of the robot that presents minor risks of collisions.

Finally, for the movement of transporting and plugging the column (Movement 4, problem $\mathbf{P4b}^R$), with the right hand, the bounce posture was selected in less than 1.3 seconds (Snapshots (J), (K), (L), (M) in Figure 1). This is also a quite challenging problem since the collision between the column that is transported by the right hand and all the surrounding obstacles must be avoided.

Figure 2 shows the generated 3D movements of the robotic arms and hands. The movements present several characteristics observed in human motor behavior. Namely, bellshaped and biphasic tangential hand velocity profiles. The later is a prominent characteristic in collision avoidance behaviours ([13], [25], [17]).

4 Conclusions and future work

In this paper we have presented a model for addressing the problem of planning collision free trajectories of a dual-arm anthropomorphic robot. Since a main motivation for this work is to guarantee human-like motion, the

Movement 1

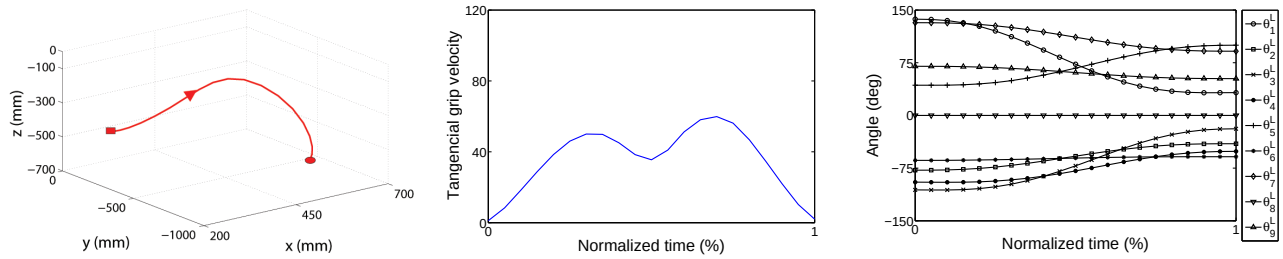

Movement 2

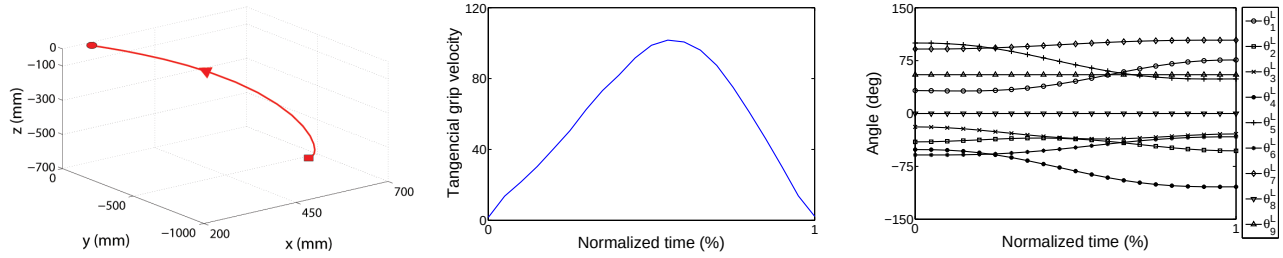

Movement 3

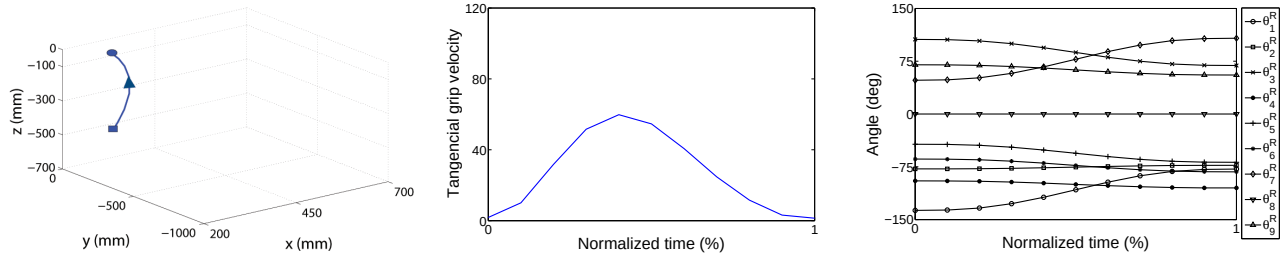

Movement 4

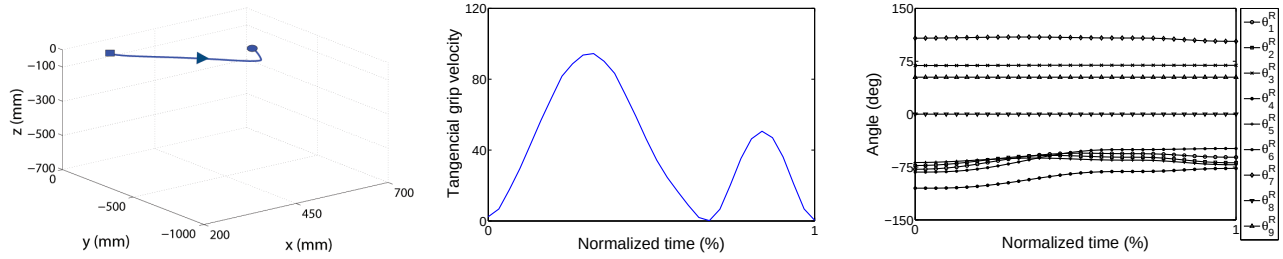

Fig. 2: From the left to the right: hand trajectory, tangential hand velocity, joint trajectories.

model takes into account important regularities and optimality principles observed in behavioral studies of human upper-limb movements. The problem was formalized as a large scale nonlinear optimization problem, which was solved using IPOPT. The model was tested as a part of the cognitive control architecture of an anthropomorphic robot in scenarios that naturally occur in human-robot collaboration, such as the joint construction of a toy object. The bimanual action planner sets desired intermediate goals for both hands, which must take into account the anticipated ultimate goal of what to do with the object. Simulation studies have shown that this model is a promising start to generate feasible and realistic hand trajectories for action sequences involving the two hands. The computational costs involved in the planning allow for real-time human-robot interaction. The robot avoids collisions of its arms and hands with its own body, the multiple objects in the scene - namely the table, the objects to be grasped and the intermediate obstacles, like the toy vehicle - as the construction proceeds. A qualitative analysis reveals that the movements of the robot exhibit basic characteristics of human movements: bell shaped and biphasic tangential hand velocity profiles - a prominent characteristic in collision avoidance behaviours ([13],[17], [25]). However, we are aware that further work needs to be performed in order to render the bimanual actions more naturalistic. Specifically, in future work we will address tasks that require the movements of the two hands to be tightly synchronized, and we will investigate different types of cost functions associated with various types of bimanual tasks (e.g. depending on the degree of asymmetry of the role of the two hands). Implementing and validating the model in the real bimanual robotic system, in tasks involving collaboration with human partners, is also an important issue which will also be addressed in future work.

Acknowledgement

This work was conducted in the scope of the EU funded Project PF7 Marie Curie “NETT - Neural Engineering Transformative Technologies”, and in addition partially supported by FCT (Foundation for Science and Technology) within the projects PEst-OE/MAT/UI0013/2014, FCOMP-01-0124-FEDER-022674 and PEst-OE/EEI/UI0319/2014.

References

[1] T. Fukuda, R. Michelini, V. Potkonjak, S. Tzafestas, K. Valavanis and M. Vukobratovic, How far away is artificial man? Robotics & Automation Magazine, IEEE **8**, 66–73 (2001).

[2] B. R. Duffy, Anthropomorphism and the social robot, Robotics and Autonomous Systems **42**, 177–190 (2003).

[3] T. Fong, I. Nourbakhsh. and K. Dautenhahn, A survey of socially interactive robots: concepts, design and applications, Robotics and Autonomous Systems **42**, 143-166 (2003).

[4] S. Schaal, The new robotics: Towards human-centered machines, HFSP Journal **1**, 115-126 (2007).

[5] S. Schaal, P. Mojaherian and A. Ijspeert, Dynamics systems vs. optimal control: A unifying view, Progress in Brain Research **165**, 425–445 (2007).

[6] E. Bicho, W. Erlhagen, L. Louro and E. Costa e Silva, Neuro-cognitive mechanisms of decision making in joint action: a Human-Robot interaction study, Human Movement Science **30**, 846–868 (2011).

[7] E. Bicho, W. Erlhagen, L. Louro, E. Costa e Silva, R. Silva and N. Hipolito, A dynamic field approach to goal inference, error detection and anticipatory action selection in human-robot collaboration, New Frontiers in HumanRobot Interaction, John Benjamins Publishing Company, 135-164 (2011).

[8] A. Edsinger and C.C. Kemp, Two arms are better than one: a behavior-based control system for assisted bimanual manipulation. Proceedings of International Conference of Advanced Robotic System, 345–355 (2007).

[9] N. Vahrenkamp, D. Berenson, T. Asfour, J. Kuffner and R. Dillmann, Humanoid motion planning for dual-arm manipulation and re-grasping tasks, Proceedings of the IEEE International Conference on Intelligent Robots and Systems, 2464-2470 (2009).

[10] C. Smith, Y. Karayiannidis, L. Nalpantidis, X. Gratal, P. Qi, D.V. Dimarogonas and D. Kragic, Dual arm manipulation - A survey, Autonomous Systems **60**, 1340–1353, (2012).

[11] F. Zacharias, C. Schlette, F. Schmidt, C. Borst, J. Rossmann and G. Hirzinger, Making planned paths look more human-like in humanoid robot manipulation planning, Proceedings of IEEE International Conference on Robotics and Automation, 1192–1196 (2011).

[12] D. Rosenbaum, R. Meulenbroek, J. Vaugham and C. Jansen, Posture-based Motion planning: Applications to grasping, Psychological Review **108**, 709–734 (2001).

[13] J. Lommertzen, E. Costa e Silva, R. Cuijpers and R.G.J Meulenbroek, Collision-avoidance characteristics of grasping: Early signs in hand and arm kinematics, Anticipatory Behavior in Adaptive Learning Systems post-conference proceedings, 188-208 (2008).

[14] N. Stepp and M.T. Turvey, On strong anticipation, Cognitive Systems Research **11**, 148–164 (2010).

[15] E. Costa e Silva, F. Costa, E. Bicho and W. Erlhagen, Nonlinear Optimization for Human-like Movements of a High Degree of Freedom Robotics Arm-hand System, Lecture Notes in Computer Science **6784**, 327–342 (2011).

[16] E. Bicho, W. Erlhagen, E. Sousa, L. Louro, N. Hipolito, E. C. Silva, R. Silva, F. Ferreira, T. Machado, M. Hulstijn, Y. Maas, E. de Bruijn, R.H. Cuijpers, R. Newman-Norlund, H. van Schie, R.G.J. Meulenbroek and H. Bekkering, The Power of Prediction: Robots that Read Intentions, Proceedings of the IEEE/RSJ International Conference on Intelligent Robots and Systems, 5458–5459 (2012).

[17] D. Rosenbaum, R. Meulenbroek, J. Vaughan and C. Jansen, Coordination of reaching and grasping by capitalizing on obstacle avoidance and other constraints, Exp Brain Res **128**, 92–100 (1999).

[18] N. Ratliff, M. Zucker, J.A. Bagnell and S. Srinivasa, CHOMP: Gradient Optimization Techniques for Efficient Motion Planning, Proceedings of IEEE Int. Conf. on Robotics and Automation, 489–494 (2009).
[19] U. Pattacini, F. Nori, L. Natale, G. Metta and G. Sandini, An experimental evaluation of a novel minimum-jerk cartesian controller for humanoid robots, Proceedings of Int. Conf. on Intelligent Robots and Systems, 1668–1674 (2010).
[20] A. Wächter and L. Biegler, On the implementation of an interior-point filter line-search algorithm for large-scale nonlinear programming, Mathematical Programming **106**, 25–57 (2007).
[21] S. Albrecht, K. Ramirez-Amaro, F. Ruiz-Ugalde, D. Weikersdorfer, M. Leibold, M. Ulbrich and M. Beetz, Imitating human reaching motions using physically inspired optimization principles, Proceedings of 11th IEEE-RAS Int. Conf. on Humanoid Robots, 602–607 (2011).
[22] M. Taïx, M.T. Tran, P. Souères and E. Guigon, Generating human-like reaching movements with a humanoid robot: A computational approach, Journal of Computational Science **4**, 269-284 (2013).
[23] E. Costa e Silva, J. P. Araújo, D. Machado, M. F. Costa, W. Erlhagen and E. Bicho, Generating human-like movements on an anthropomorphic robot using an interior point method, AIP Conference Proceedings **1558**, 602–605 (2013).
[24] J.J. Craig, Introduction to robotics: mechanics and control. 2nd ed., Addison-Wesley, (1998).
[25] J. Dean and M. Brüwer, Control of human arm movements in two dimensions: paths and joint control in avoiding simple linear obstacles, Experimental Brain Research **97**, 497–514 (1994).

Eliana Costa e Silva received her MSc in Mathematics and Applications and a PhD in the area of Automation and Robotics (PhD program on Electronics and Computers Engineering) at University of Minho, in 2005 and 2011, respectively. In 2009 she took a specialized formation course in Optimization Applied to Sciences and Engineering. She was a research assistant at the European projects ”Artesimit - Artefact Structural Learning Through Imitation” and ”JAST-Joint Action Science and Technology”. Her research interests are Autonomous and Anthropomorphic Robots, nonlinear constrained optimization and numerical methods. Currently she is an invited professor at ESTGF-Polytechnic Institute of Porto, Portugal

M. Fernanda P. Costa is Assistant Professor at the Department of Mathematics and Applications and Researcher in the Centre of Mathematics from the University of Minho (Portugal). She received the PhD degree in Mathematics at University of Minho (2002). Her research interests are in Nonlinear Programming, Global Optimization, Derivative-Free Methods, Filter Methods, and Mixed-Integer Nonlinear Optimization.

Jos P. Arajo received his Msc in Industrial Electronics and Computers Engineering, with specialization on ”Automation, Control and Robotics” and ”Microelectronics” at the University of Minho, Portugal, in 2013. During the same year he also finished his master dissertation entitled ”From Unimanual to Bimanual Manipulation in the Anthropomorphic Robot ARoS”. His research interests are focused on Automation, Non-linear Dynamical Systems, Programming, Simulation and Robotics. Currently he is working at Novabase Portugal.

Drio Machado received his Msc in Industrial Electronics and Computers Engineering, with specialization on ”Automation, Control and Robotics” and ”Microelectronics” at the University of Minho, Portugal, in 2013. During the same year he also finished his master dissertation entitled ”From tele-operation to helpful robotic team-mates”. His research interests are focused on Automation, Non-linear Dynamical Systems, Programming, Simulation and Robotics.

Luis Louro received a PhD in the area of Automation and Robotics (PhD program on Electronics and Computers Engineering) at University of Minho, in 2010. He was a research assistant at the European projects ”Artesimit - Artefact Structural Learning Through Imitation” and ”JAST-Joint Action Science and Technology”. His research interests are Autonomous and Anthropomorphic Robotics, Human-Robot Interaction. Currently he is he has a post-doc position at the University of Minho, Portugal, and he is an assistant professor at Lusada University, Portugal.

Wolfram Erlhagen is Associate Professor at the Department of Mathematics and Applications at the University of Minho, Portugal. He has been PI in several European (FP6 & FP7) and national projects in the ICT topic. His multidisciplinary research covers the multi-scale analysis of neuronal activity, the functional modelling of brain circuits, and the implementation of neuro-based models in autonomous robots. In close cooperation with partners in industry and healthcare, he uses the results of the fundamental research to develop innovative solutions for problems in human-robot interactions in general, and the flexible control of high-DOF robotics systems in particular.

Estela Bicho is Associate Professor at the Department of Industrial Electronics at University of Minho, Portugal, where she is responsible for courses in Non-linear Dynamical Systems, Control and Robotics and heads the research lab on Autonomous (mobile and anthropomorphic) Robotics & Dynamical systems. She is also a staff member of the MIT—Portugal Joint Program on Advanced Studies in Bioengineering. She obtained the PhD degree in Robotics, Automation and Control, in 1999, from the University of Minho. Her PhD work received the honour price from Portuguese-IBM (1999). Her research concentrates on the use of dynamical systems for the design and implementation of neuro-cognitive control architectures for flexible control of high-DOF robotics systems, including Human-robot interaction. She has been PI in several national and EU funded research projects in robotics.